

# Multinuclear NMR Study of the Aggregates between Methyllithium and Lithium Bromide in Toluene

Stéphanie Desjardins,<sup>†</sup> Karine Flinois,<sup>†</sup> Hassan Oulyadi,<sup>†</sup> Daniel Davoust,<sup>†</sup>  
Claude Giessner-Prettre,<sup>‡</sup> Olivier Parisel,<sup>‡</sup> and Jacques Maddaluno<sup>\*,†</sup>

*Institut de Recherche en Chimie Organique Fine, UMR 6014 CNRS, Université de Rouen,  
76821 Mont St Aignan Cedex, France, and Laboratoire de Chimie Théorique,  
UMR 7616 CNRS, Université Pierre & Marie Curie, 4 Place Jussieu,  
75252 Paris Cedex 05, France*

Received March 19, 2003

A set of high-field, low-temperature NMR experiments has been conducted on various mixtures of Me<sup>6</sup>Li and <sup>6</sup>LiBr in toluene. All the <sup>6</sup>Li and <sup>1</sup>H signals of the (MeLi)<sub>n</sub>(LiBr)<sub>4-n</sub> aggregates were unambiguously assigned via one- and two- dimensional (HOESY and COSY) experiments. The influence of the MeLi/LiBr ratio on the concentration of these different aggregates in solution was then studied. The data suggest that the populations of the five possible complexes follow an almost purely statistical distribution with the exception of the MeLi(LiBr)<sub>3</sub> species. The later, which was found to be less abundant than expected, is also less favored on the basis of aggregation energies obtained from density functional theory calculations.

## Introduction

The influence of lithium halides on the reactivity of organometallic reagents, in general, and on organolithium compounds, in particular, has been the subject of many reports in the literature.<sup>1</sup> The effect of such halides is generally attributed to the modification of the aggregation pattern of the species in solution; however the details of the changes in the complexes remain generally unknown. The formation of mixed-aggregates between alkyllithium compounds and lithium bromide or iodide was demonstrated in 1960 in the solid state<sup>2</sup> and in 1967 in solution.<sup>3</sup> A <sup>7</sup>Li/<sup>1</sup>H NMR pioneer study published as early as 1972 by Novak and Brown<sup>4</sup> provided a detailed description of the tetrameric aggregates formed between methyllithium and lithium bromide in diethyl ether at various temperatures and for different MeLi/LiBr ratios. These authors concluded that five different types of mixed tetramers can arise, following the general formula (MeLi)<sub>4-n</sub>(LiBr)<sub>n</sub> with *n* = 0–4, for which the relative abundances depend explicitly on the MeLi/LiBr ratio. Unfortunately, the relatively broad lines due to the large contribution of the quadrupolar relaxation of the <sup>7</sup>Li nucleus and the

low resolution associated with the 220 MHz instrument used in Brown's work prevented the observation of the eight signals expected for the various lithium cations belonging to these aggregates. The relative intensities of the four signals corresponding to the four possible lithium local environments (that is, different first neighbors, Figure 1) had thus been measured, but the exact population of the five different tetramers (A–E) could not be determined: the weak effect of the remote ligand induces chemical shift differences smaller than the resolution of Brown's instrument.

For instance, the <sup>7</sup>Li NMR is unable to discriminate between Li<sup>3</sup> (belonging to a B-type complex) and Li<sup>4</sup> (included in a C-type one), for which only the remote ligand is different. Repeating these experiments with a <sup>6</sup>Li-marked alkyllithium compound and a high-field instrument is likely to give better-resolved signals. Eppers and Günther have previously shown the advantages of this "isotopes switch" in a study relying on the simple differences between <sup>6</sup>Li signal intensities due to NOE effects with neighbor <sup>1</sup>H.<sup>5</sup> This fine work was completed by a careful description of mixed aggregates involving CH<sub>3</sub>Li, CD<sub>3</sub>Li, and LiI (in a fixed 1:1:2 ratio) at 178 K in diethyl ether. The results led the authors to conclude that (i) at this temperature, the inter- and intra-aggregate exchanges are slow and (ii) the five possible tetramers A–D coexist in solution in proportions consistent with a statistical distribution. Only the <sup>6</sup>Li spectra were reported, although the <sup>1</sup>H signals could, in principle, also be used to differentiate the various complexes. However, all methyl groups are equivalent in a given tetramer (Figure 1), and thus only four different signals can be expected for the five tetramers, while a precise assay of the species requires a baseline separation between signals and therefore a relatively large chemical shift range.

\* Corresponding author. Fax: (33) 235 522 971. E-mail: jmaddaluno@crihan.fr.

<sup>†</sup> IRCOF, Université de Rouen.

<sup>‡</sup> LCT, Université Paris VI.

(1) See for instance: (a) Murakata, M.; Nakajima, M.; Koga, K. *J. Chem. Soc., Chem. Commun.* **1990**, 22, 1657. (b) Yasukata, T.; Koga, K. *Tetrahedron: Asymm.* **1993**, 4, 35. (c) Seebach, D.; Bossler, H. G.; Flowers, R.; Arnett, E. M. *Helv. Chim. Acta* **1994**, 77, 291. (d) Asensio, G.; Aleman, P. A.; Domingo, L. R.; Medio-Simón, M. *Tetrahedron Lett.* **1998**, 39, 3277. (e) Murakata, M.; Yasukata, T.; Aoki, T.; Nakajima, M.; Koga, K. *Tetrahedron* **1998**, 54, 2449. (f) Sosa-Rivadeneira, M.; Muñoz-Muñiz, O.; Anaya de Parrodi, C.; Quintero, L.; Juaristi, E. *J. Org. Chem.* **2003**, 68, 2369.

(2) Glaze, W.; West, R. *J. Am. Chem. Soc.* **1960**, 82, 4437.

(3) Waack, R.; Doran, M. A.; Baker, E. B. *J. Chem. Soc., Chem. Commun.* **1967**, 1291.

(4) Novak, D. P.; Brown, T. L. *J. Am. Chem. Soc.* **1972**, 94, 3793.

(5) Eppers, O.; Günther, H. *Helv. Chim. Acta* **1990**, 73, 2071.

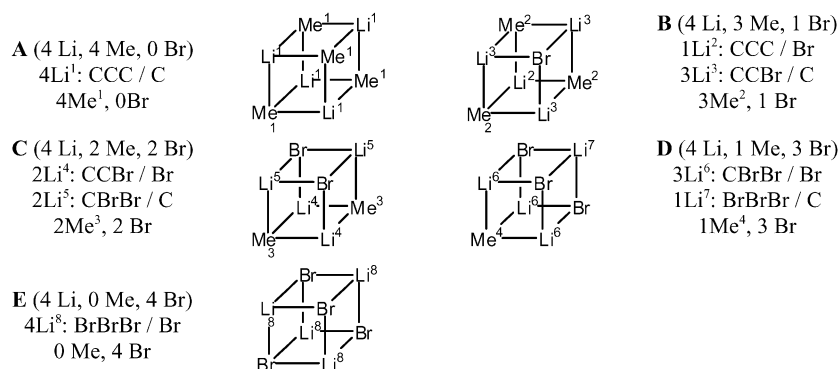


**Figure 1.** Five different tetramers involving methyllithium and lithium bromide. The different lithium nuclei are characterized by their first/remote ligands. For instance, in complex C, the notation 2Li<sup>4</sup>: CCB/Br means that type-4 lithiums are directly surrounded by two carbons and one bromine and indirectly by one remote bromine ligand.

We present here results obtained with methyllithium and lithium bromide in a 75:25 *o*-toluene–diethyl ether (DEE) mixture. The DEE comes from the methyllithium synthesis (see the Experimental Details section) and ensures the solubility of both MeLi and LiBr. A similar reaction medium was actually used in a previous study of the enantioselective protonation of tetralone lithium enolates.<sup>6</sup> We have focused here on the measurement of the evolution of the population of the various aggregates as a function of the MeLi/LiBr ratio through <sup>6</sup>Li labeling and “standard” high-field NMR. Such an analysis can be important for correlating the observed reactivity/selectivity to the distribution of aggregates.<sup>1,6</sup>

## Results and Discussion

**Identification of the Species in Solution.** To optimize the experimental conditions, we first considered the effect of temperature on a representative sample of MeLi/LiBr = 1:1.6. Decreasing the temperature from 298 to 195 K induces a progressive splitting of the original <sup>1</sup>H and <sup>6</sup>Li singlets into three and seven main signals, respectively (Figure 2). It also transforms the <sup>13</sup>C singlet into a superposition of two to three multiplets. Since a temperature less than 200 K is required to reach a sufficient level of resolution, we chose to work at 183 K (with one exception mentioned below), that is, in conditions similar to those employed by Günther.<sup>5</sup>

At this temperature, the <sup>1</sup>H spectrum of a pure methyllithium solution displays one singlet at –1.51 ppm (Figure 3A). The corresponding <sup>6</sup>Li recording also exhibits one singlet at 2.99 ppm, together with a set of weak unidentified broad signals around 1.5 ppm. The <sup>13</sup>C spectrum features a heptet around –13.7 ppm with <sup>1</sup>J(<sup>13</sup>C,<sup>6</sup>Li) = 5.9 Hz. The empirical Bauer–Winchester–Schleyer (BWS) formula<sup>7</sup> gives access to the number of <sup>6</sup>Li nearest neighbors (*n*):

$$^1J(^{13}\text{C}, ^6\text{Li}) \approx (17 \pm 2)/n$$

The measured value suggests here that *n* ≈ 3. Both the static tetramers and hexamers have three lithium nuclei around each carbon. Tetramers have been ob-

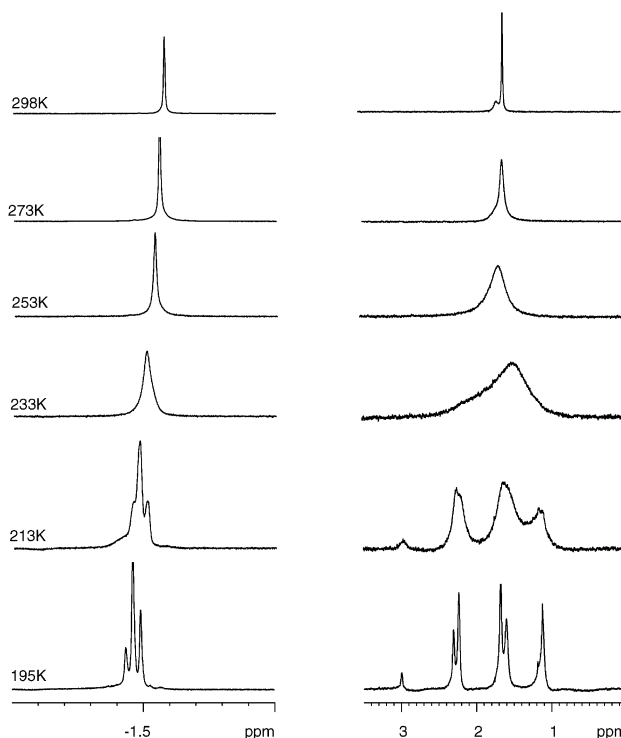


**Figure 2.** Temperature effect (298–195 K) on <sup>1</sup>H (left) and <sup>6</sup>Li (right) NMR spectra of a MeLi/LiBr = 1:1.6 solution in toluene.

served for instance by Brown in diethyl ether<sup>4</sup> and McKeever in THF,<sup>8</sup> while hexamers have been described by Fraenkel for *s*-BuLi and *n*-PrLi in cyclopentane<sup>9</sup> and by Thomas for several alkylolithiums in the same solvent.<sup>10</sup> The splitting of the <sup>13</sup>C resonance due to the <sup>13</sup>C–<sup>6</sup>Li coupling in organolithium hexamers observed to be ca. 3.0 Hz is actually the result of a fast first-order reorganization of the aggregate which averages the three one-bond <sup>13</sup>C–<sup>6</sup>Li coupling constants (ca. 6 Hz) with very small couplings to the three distant <sup>6</sup>Li's.<sup>10</sup> Therefore, the tetramer is the most likely form of aggregation under our conditions, and the 2.99 ppm

(8) McKeever, L. D.; Waack, R.; Doran, M. A.; Baker, E. B. *J. Am. Chem. Soc.* **1968**, *90*, 3244.

(9) (a) Fraenkel, G.; Henrichs, M.; Hewitt, J. M.; Su, B. M.; Geckle, M. J. *J. Am. Chem. Soc.* **1980**, *102*, 3345. (b) Fraenkel, G.; Henrichs, M.; Hewitt, M.; Su, B. M. *J. Am. Chem. Soc.* **1984**, *106*, 255.

(10) Thomas, R. D.; Jensen, R. M.; Young, T. C. *Organometallics* **1987**, *6*, 565.

(6) (a) Flinois, K. Ph.D. Thesis, Université de Rouen, 2000. (b) Flinois, K.; Yuan, Y.; Bastide, C.; Harrison-Marchand, A.; Maddaluno, J. *Tetrahedron* **2002**, *58*, 4707.

(7) Bauer, W.; Schleyer, P. von R. *Adv. Carbohydr. Chem.* **1992**, *1*, 89.

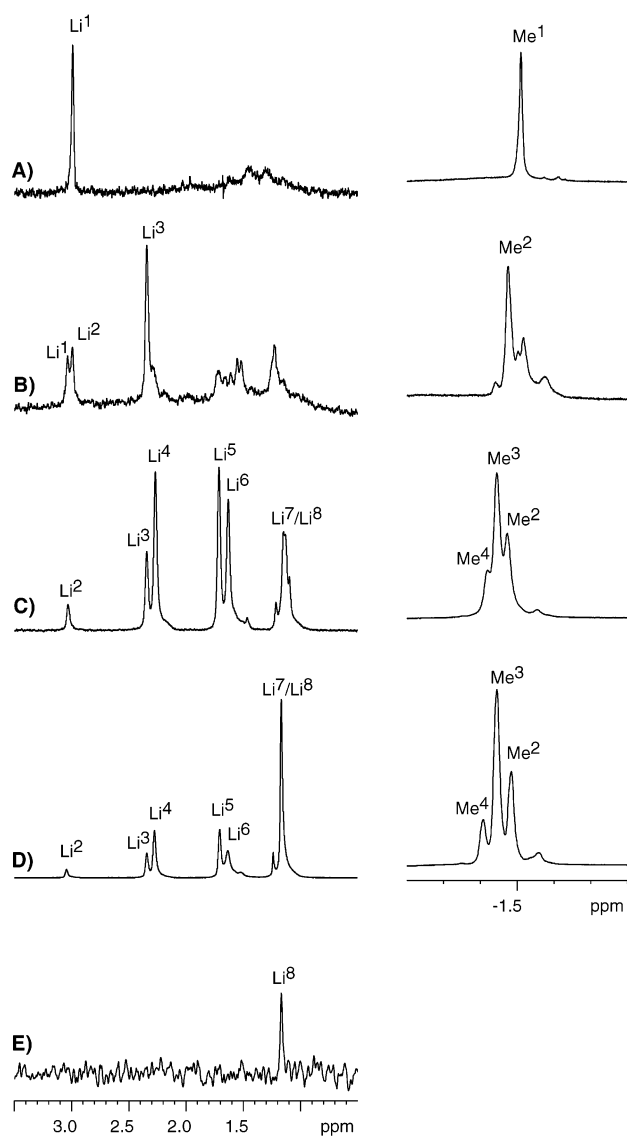


**Figure 3.**  $^1\text{H}$  (left),  $^6\text{Li}$  (middle), and  $^{13}\text{C}$  (right) NMR spectra at  $T = 183\text{ K}$  of  $\text{Me}^6\text{Li}$  in toluene after addition of  $^6\text{LiBr}$ : (A) pure  $\text{MeLi}$ ; (B)  $\text{MeLi/LiBr} = 2:1$ ; (C)  $\text{MeLi/LiBr} = 1:1.4$ ; (D)  $\text{MeLi/LiBr} = 1:3$ ; (E) pure  $\text{LiBr}$ .

lithium singlet is to be associated with  $\text{Li}^1$  in the  $(\text{MeLi})_4$  aggregate (species A in Figure 1).

The first addition of  $\text{LiBr}$  has been adjusted to a  $\text{MeLi/LiBr} = 2:1$  ratio, and the associated spectra are displayed in Figure 3B. The most interesting aspect of the data is the  $^6\text{Li}$  resonance, which displays, besides the original singlet (slightly shifted in this sample to 3.03 ppm), two additional sharp signals at 2.99 and 2.34 ppm, for which the relative integration, after deconvolution, is 1:2.8. Unresolved multiplets are also observed at higher field. We interpret this result as the formation of a dominant B-type mixed aggregate for which the  $\text{Li}^2$ -type cation corresponds to the 2.99 ppm signal and the  $\text{Li}^3$ -type cation to the 2.34 ppm singlet. This preliminary hypothesis is based on (i) the expected similarity between the chemical shifts of  $\text{Li}^1$  (in complex A, Figure 1) and  $\text{Li}^2$  (in complex B), differing only by the remote ligand effect, and (ii) the ratio between the  $\text{Li}^2$  and  $\text{Li}^3$  signal integration being close to 3, as expected in complex B. The  $^1\text{H}$  spectrum is difficult to interpret at this stage since it features a broad signal corresponding

to several species. However, the highest peak at  $-1.47$  ppm is probably characteristic of the methyl in complex B, as verified by the HOESY experiment discussed below. By analogy, the peak at  $-1.52$  ppm is associated with the methyl groups in tetramer A.

A second addition of  $\text{LiBr}$ , which decreases the  $\text{MeLi/LiBr}$  ratio to 1:1.4, yields a clear set of singlets (Figure 3C). While the  $\text{Li}^1$  peak at low field vanishes, four new signals appear in addition to the 2.99 and 2.34 ppm ones, corresponding to  $\text{Li}^2$  and  $\text{Li}^3$ : (i) two strongly peaked singlets of equal intensity at 2.27 and 1.71 ppm that have been assigned to  $\text{Li}^4$  (as expected, similar to the  $\text{Li}^3$  chemical shift) and  $\text{Li}^5$ , respectively, in the newly formed complex C; (ii) a sharp singlet at 1.63 ppm, assigned to  $\text{Li}^6$  from a D-type complex; (iii) a large singlet at 1.17 ppm that likely incorporates the corresponding  $\text{Li}^7$  signal together with one or several aggregates of pure  $\text{LiBr}$  (including  $\text{Li}^8$ ). The  $^1\text{H}$  spectrum displayed three main singlets, likely associated with the aggregates identified by the  $^6\text{Li}$  spectrum, viz., B (at  $-1.47$  ppm, as above), C (at  $-1.44$  ppm), and D (at  $-1.42$  ppm). These assignments, based on chemical shifts and integration arguments similar to those above, were also checked by a HOESY two-dimensional spectrum (vide infra).

Further addition of  $\text{LiBr}$  decreases the  $\text{MeLi/LiBr}$  ratio to 1:3. The  $^6\text{Li}$  spectrum in Figure 3D shows the same collection of peaks. Now, however, the peak at the highest field (1.05 ppm) is dramatically increased, while the ratio between the other signals remains more or less the same. Within the framework of the above assignments, this strongly peaked signal likely corresponds to the  $\text{Li}^8$  in pure  $\text{LiBr}$  tetramers E, with the complexes B, C, and D remaining in fixed relative concentrations. Similarly, the  $^1\text{H}$  spectrum exhibits the same three main signals in comparable ratios.

Finally, we have also recorded the  $^6\text{Li}$  spectrum of our stock solution of  $^6\text{LiBr}$  in ether, dissolved in  $d_8$ -toluene as above (Figure 3E). The low solubility of  $\text{LiBr}$  in toluene gives a weak singlet at 1.14 ppm, a chemical shift similar to that observed for the main species in the above spectrum.

All the above assignments could be confirmed by performing  $^6\text{Li}$ - $^1\text{H}$  HOESY (Figure 4A) and  $^6\text{Li}$ - $^6\text{Li}$  COSY experiments (Figure 4B) on a  $\text{MeLi/LiBr} = 1:1.6$  sample at 195 K. The first spectrum clearly shows the two correlations between  $\text{Me}^2$  and both  $\text{Li}^2$  and  $\text{Li}^3$  signals, indicating that these three species belong to the same aggregate. The same observation could be made for  $\text{Me}^3$ ,  $\text{Li}^4$ , and  $\text{Li}^5$ , on one hand, and for  $\text{Me}^4$ ,  $\text{Li}^6$ , and  $\text{Li}^7$  on the other. Thus, these data fully support the assignments made above from the relative intensities of the lithium and proton signals. Interestingly, the COSY long-range experiment shows a fine  $\text{Li}^2/\text{Li}^3$  correlation but no  $\text{Li}^4/\text{Li}^5$  and  $\text{Li}^6/\text{Li}^7$  cross-peaks. This absence can be understood in light of recent results by Hilmersson and co-workers.<sup>11</sup> These authors have observed that in heterogeneous aggregates involving lithium amides and alkyl lithium compounds, a  $^2J(^6\text{Li}, ^6\text{Li})$  coupling can be measured between nonequivalent lithium nuclei belonging to a quadrilateral only if the two complementary atoms are carbons. This feature is found

(11) Arvidsson, P. I.; Ahlberg, P.; Hilmersson, G. *Chem. Eur. J.* **1999**, *5*, 1348.

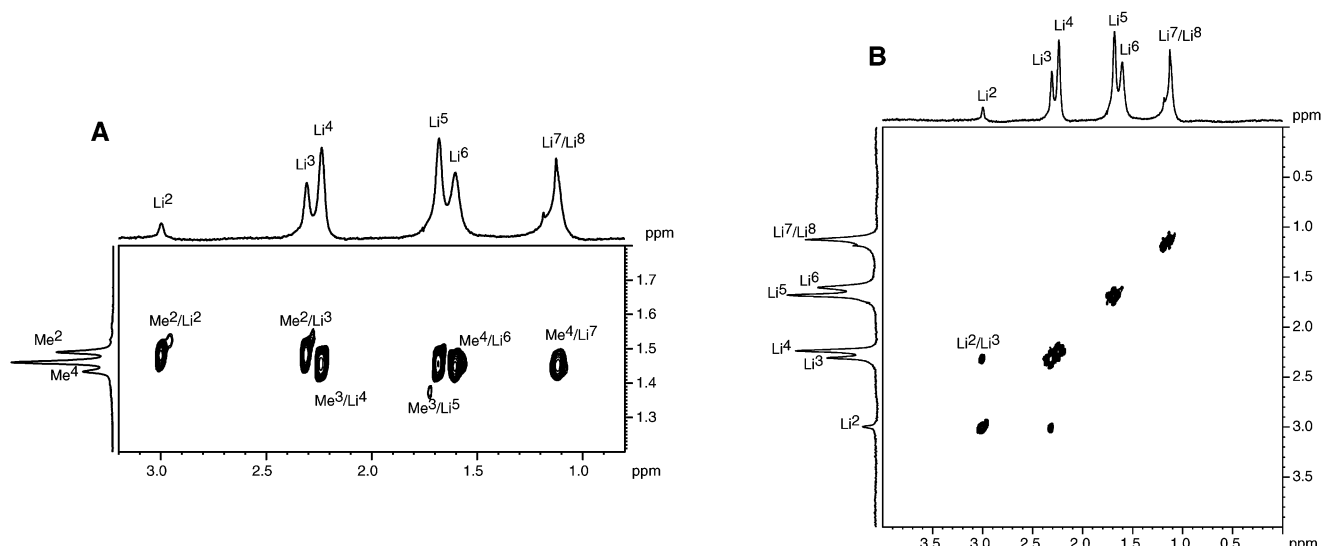


**Figure 4.** Bidimensional  ${}^6\text{Li}$ ,  ${}^1\text{H}$  HOESY (left) and  ${}^6\text{Li}$ ,  ${}^6\text{Li}$  COSY (right) of a 1:1.6  $\text{Me}^6\text{Li}/{}^6\text{LiBr}$  solution in toluene at 195 K.

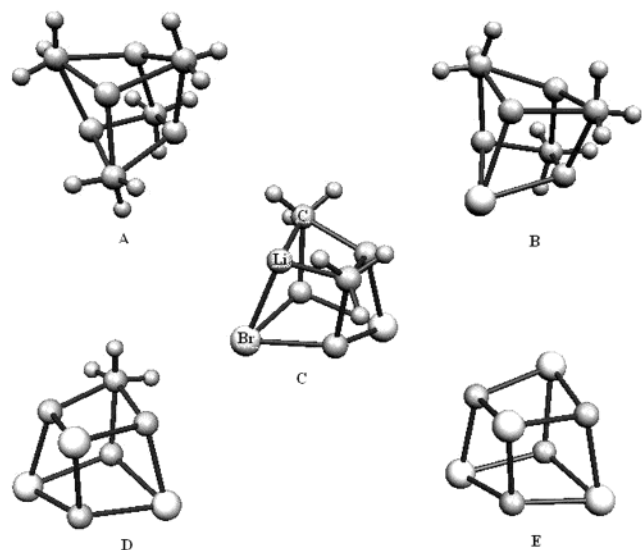


**Figure 5.** DFT optimized  $(\text{MeLi})_n(\text{LiBr})_{4-n}$  tetramers A–E.

exclusively in complex B, which justifies the sole  $\text{Li}^2/\text{Li}^3$  correlation. Worthy of note is the case of complex D, in which  $\text{Li}^6$  and  $\text{Li}^7$  share three faces completed by two bromine atoms. Moreover, no  $\text{Li}^6/\text{Li}^7$  cross-peaks are observed in the spectrum of Figure 4B, suggesting that Hilmersson's observation can be extended to other heterogeneous aggregates.

We decided to investigate the origin of this phenomenon by computing the  ${}^6\text{Li}$ – ${}^6\text{Li}$  coupling constants for lithium atoms belonging to mixed tetramers B, C, and D. We first ran a complete optimization of the five tetramers, yielding the structures depicted in Figure 5. Obviously, the final polyhedra are far from the ideal cubes of Figure 1. The Li–Li coupling constants, calculated either at the Hartree–Fock (HF) or density functional theory (DFT) levels, are reported in Table 1, together with the corresponding distances. The coupling between nonequivalent lithium nuclei (bold values in the table), the only ones to be observed, decrease from B to C to D at the HF level. This result is consistent with the observation of a  $\text{Li}^2/\text{Li}^3$  COSY correlation and

**Table 1.** Hartree–Fock (HF) and DFT Calculated  ${}^6\text{Li}$ – ${}^6\text{Li}$  Distances and Coupling Constants in Tetramers B, C, and D (Figures 1 and 5)<sup>a</sup>

	HF				DFT	
	6-31G**		6-31+G**		B3P86/6-31+G**	
	$d_{\text{Li-Li}}$ (Å)	$J$ (Hz)	$d_{\text{Li-Li}}$ (Å)	$J$ (Hz)	$d_{\text{Li-Li}}$ (Å)	$J$ (Hz)
<b>Tetramer B</b>						
$\text{Li}^2$ – $\text{Li}^3$	2.42	<b>–0.86</b>	2.42	<b>–0.72</b>	2.42	<b>–0.60</b>
$\text{Li}^3$ – $\text{Li}^3$	2.60	–0.39	2.59	–0.54	2.59	–0.52
<b>Tetramer C</b>						
$\text{Li}^4$ – $\text{Li}^4$	2.44	–0.77	2.44	–0.82	2.44	–0.73
$\text{Li}^4$ – $\text{Li}^5$	2.64	<b>–0.47</b>	2.64	<b>–0.65</b>	2.64	<b>–0.65</b>
$\text{Li}^5$ – $\text{Li}^5$	2.88	–0.10	2.88	–0.24	2.88	–0.25
<b>Tetramer D</b>						
$\text{Li}^6$ – $\text{Li}^7$	2.95	<b>–0.11</b>	2.96	<b>–0.20</b>	2.96	<b>–0.20</b>
$\text{Li}^6$ – $\text{Li}^6$	2.66	–0.48	2.66	–0.68	2.66	–0.64

<sup>a</sup> Bold values correspond to couplings between nonequivalent lithium nuclei.

the absence of  $\text{Li}^4/\text{Li}^5$  and  $\text{Li}^6/\text{Li}^7$  cross-coupling peaks (Figure 4), a consequence of the relatively long distance between these nuclei (2.64 and 2.96 Å, respectively, compared to 2.42 Å for  $\text{Li}^2$ – $\text{Li}^3$ ). In fact, the data in Table 1 indicate that the coupling constants computed at the HF level decrease rapidly with the inter-nuclei distances, a phenomenon that likely underlies also the observation of Hilmersson. In addition, we want to point out that the introduction of diffuse functions on non-hydrogen atoms does not affect the geometry of the complexes, yet does not account as accurately for the decrease in coupling constants from B to C to D. Taking into account the correlation, using DFT, does not significantly improve the results. The only coupling constant that could be measured is the  $\text{Li}^2$ – $\text{Li}^3$  coupling in tetramer B, suggesting that the calculated  $J$  data are overestimated. This correlation-independent discrepancy could be due to the absence of solvent in our models.

We conclude the present discussion with the  ${}^{13}\text{C}$  spectrum of Figure 6 (recorded, in this case, at 173 K). Apart from the weak methyl lithium multiplet at –12.18 ppm, only the toluene (at 137.27, 128.75, 127.91, 125.06, and 20.40 ppm) and ether (at 65.80 and 15.21 ppm) signals are observed. Interestingly, the two diethyl ether

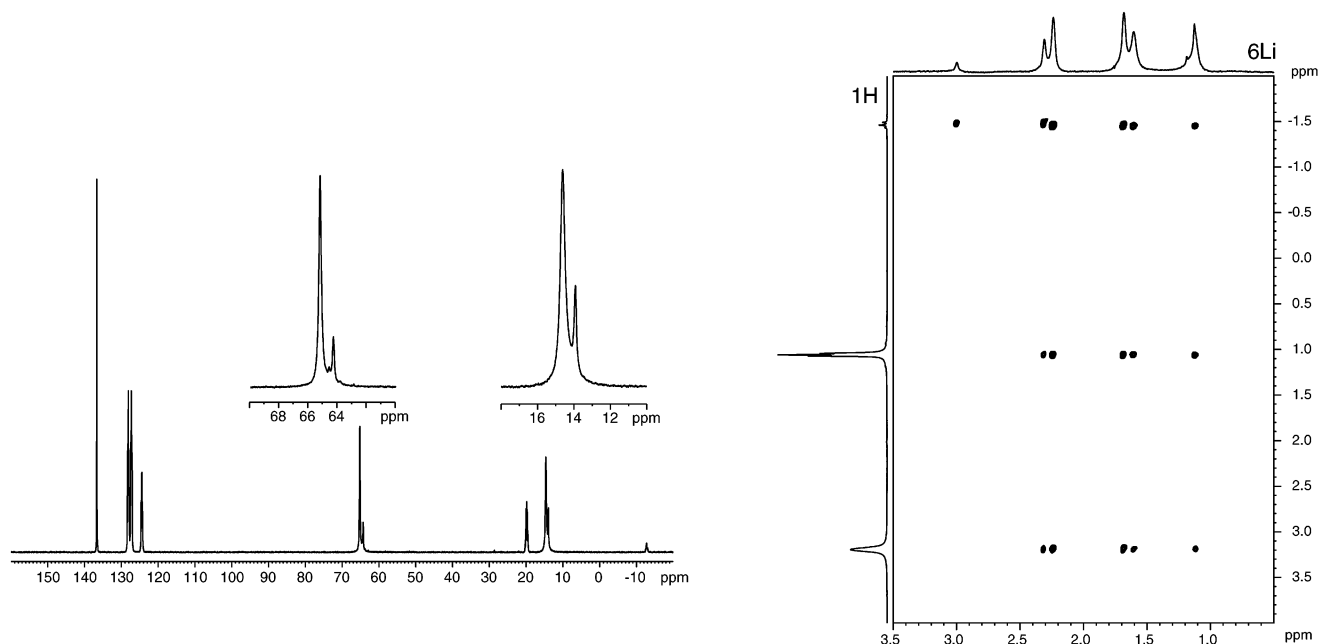


**Figure 6.**  $^{13}\text{C}$  spectrum (left, at 173 K) and HOESY (right, at 183 K) of a MeLi/LiBr = 1:1.6 sample.

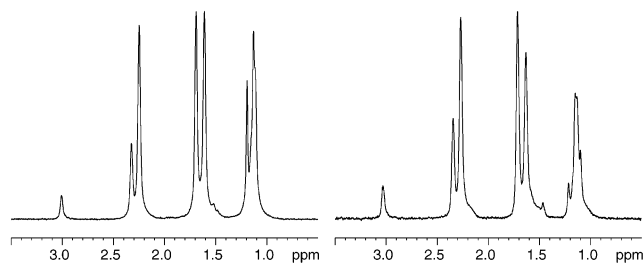


**Figure 7.**  $^6\text{Li}$  NMR spectra of a MeLi/LiBr = 1:1.4 toluene solution. Concentration = 1.1 M (left) and 0.3 M (right).

singlets are associated with two smaller peaks at high field (65.07 and 14.51 ppm). We think these new signals correspond to the  $\text{Et}_2\text{O}$  molecules directly bound to the lithium cations, i.e., in the first solvation shell, that are, at this low temperature in toluene medium, in slow exchange with free ether. This observation is supported by dipolar correlations between lithium signals and ether protons (Figure 6 right). Only in a few similar cases have slow solvent exchanges been reported before.<sup>12</sup> In the case of dimeric hexamethyldisilazide, several solvation patterns could even be characterized in ether/THF solvents.<sup>12b</sup> We did not extend our own studies in this direction yet.

**Populations in Solution.** Both the  $^1\text{H}$  and the  $^6\text{Li}$  peak assignments, made above for each complex, give access to the A/B/C/D ratio in the various cases studied. First, the influence of the absolute concentration on the relative proportions of these aggregates was checked. We recorded the  $^6\text{Li}$  and  $^1\text{H}$  spectra of a MeLi/LiBr = 1:1.4 mixture prepared either in the usual conditions or diluted three times with  $d_8$ -toluene. The spectra (Figure 7) show that there is a limited influence of the concentration on the populations.

The relative populations can be discerned from the  $^1\text{H}$  or from the  $^6\text{Li}$  data. While the  $^1\text{H}$  spectra give access

**Table 2. Proportions between Complexes A–E at Various MeLi/LiBr Ratios at 183 K as Obtained by  $^6\text{Li}$  and  $^1\text{H}$  Signal Integrations or Calculated**

MeLi/LiBr	$^1\text{H}$ ratios (A/B/C/D)	$^6\text{Li}$ ratios (A/B/C/D/E)	theoretical ratios (A/B/C/D/E)
1/0	100/0/0/0	100/0/0/0/0	100/0/0/0/0
1/0.5	28/69/3/0	18/54/28/0/0	20/40/29/10/1
1/1.4	0/23/59/18	0/12/39/24/25	3/17/36/33/11
1/3	0/20/60/20	0/8/28/19/45	0/5/21/42/32
1/ $\infty$		0/0/0/0/100	0/0/0/0/100

only to A–D, the  $^6\text{Li}$  data include the contribution of pure LiBr (complex E and higher oligomers). The poised integrations correspond, after deconvolution of the peaks, to the ratios reported in Table 2. These data, displayed in Figure 8, can be compared to those calculated within the framework of a thermodynamic equilibrium between tetramers having the same free energy of formation. Under such conditions, the fractional quantity  $F$  of each static tetramer is expected to follow the formula<sup>4</sup>

$$F_{(\text{Li}_4\text{Me}_{4-n}\text{Br}_n)} = f^{4-n}_{(\text{MeLi})} \times f^n_{(\text{LiBr})} \times \left[ \frac{4!}{(n!(4-n)!)} \right]$$

where  $n$  is the number of bromine(s) in the complex considered, and  $f^{4-n}_{(\text{MeLi})}$  and  $f^n_{(\text{LiBr})}$  are the fractional concentrations of MeLi and LiBr in the initial mixture, i.e.,  $f^{4-n}_{(\text{MeLi})} + f^n_{(\text{LiBr})} = 1$ .

The theoretical data match the spectroscopic data well. Generally, the agreement with the  $^6\text{Li}$  results is better than those from the  $^1\text{H}$  measurements. This is likely due to the high resolution and splitting of the  $^6\text{Li}$  spectra, which increases the accuracy of the measurements. It is worth underscoring the fact that the concentration of complex D is systematically smaller than expected, an observation fully consistent with Brown's results<sup>4</sup> and related to the higher energy of formation of this complex, as presented below in the theoretical results section.

DFT theoretical calculations have been performed to understand the discrepancies arising between the ex-

(12) See for instance: (a) Lucht, B. L.; Collum, D. B. *J. Am. Chem. Soc.* **1994**, *116*, 6009. (b) Lucht, B. L.; Collum, D. B. *J. Am. Chem. Soc.* **1995**, *117*, 9863. (c) Hilmersson, G. *Chem. Eur. J.* **2000**, *6*, 3069.

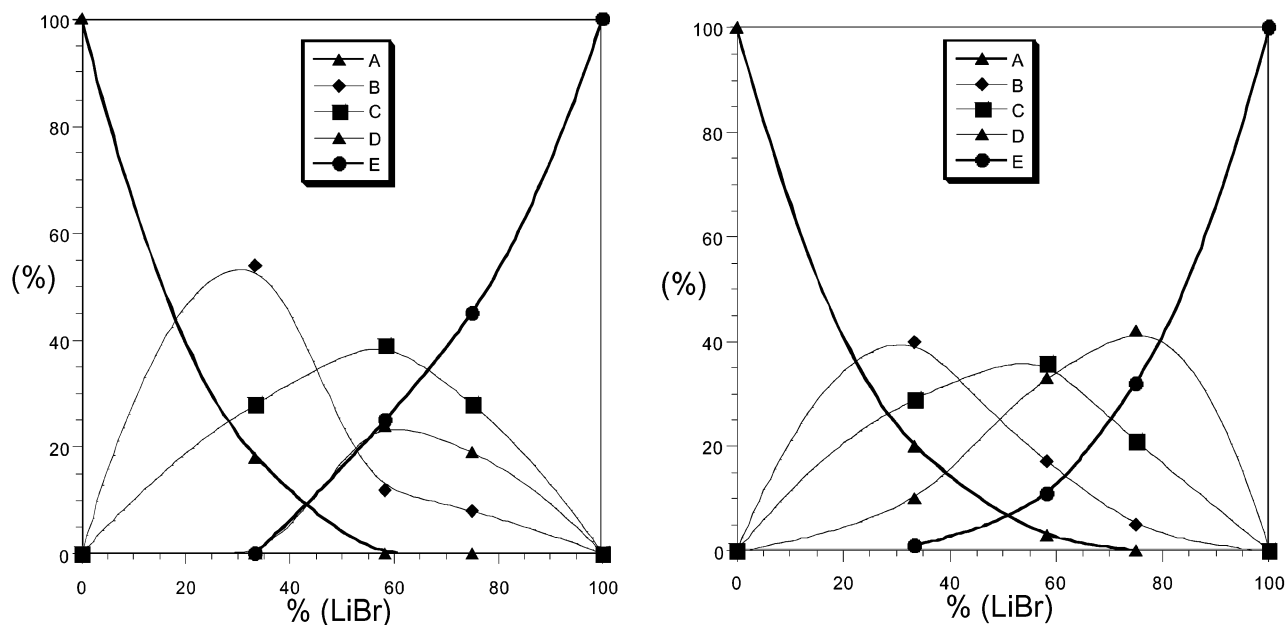


**Figure 8.** Experimental (based on  $^6\text{Li}$  NMR signal integrations, left) and statistical (right) distribution of complexes A–E as a function of LiBr molar proportion in the MeLi/LiBr mixture.

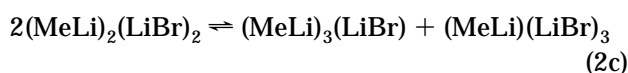
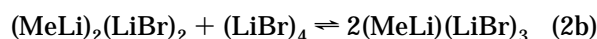
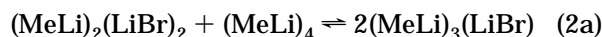
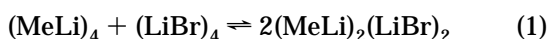
**Table 3. Energetics of Tetramers A–E in Vacuo and in Diethyl Ether (DEE)<sup>a</sup>**

tetramer	$E$ (gas-phase)	$E$ (DEE)	ZPE (kcal/mol)	$E_{\text{tot}}$ (DEE)
A	-190.665812	-190.665791	88.3	-190.525074
B	-2722.922362	-2722.923185	68.2	-2772.814500
C	-5255.180245	-5255.181041	48.7	-5255.103431
D	-7787.431533	-7787.432183	21.1	-7787.388996
E	-10319.686098	-10319.686098	6.3	-10319.67605

<sup>a</sup> Absolute energies are in atomic units.

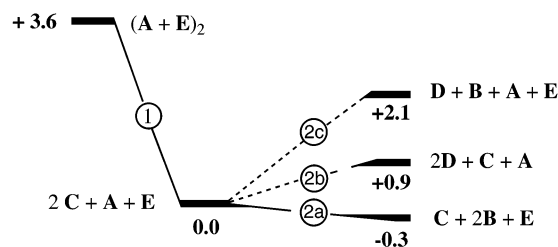
perimentally determined distributions of the five different tetramers and those predicted on the basis of statistical considerations. The energies in the gas phase and in diethyl ether are reported in Table 3, together with the zero-point energies (ZPE). The latter must be included because of its large variations among the various cases considered.

As the aggregates identified in the medium are tetramers, we have assumed that all steps in the reaction schemes leading to the final aggregates involve only mixed or pure tetramers reacting *face-to-face*. Consequently, the following steps have been considered in order to generate all possible aggregates starting from pure methyllithium and LiBr, as achieved experimentally:



The energetics of these reactions, including ZPE and solvent effects, are reported together in Scheme 1. Step 1 is clearly exothermic (3.6 kcal/mol) and favors the formation of  $(\text{MeLi})_2(\text{LiBr})_2$ . Among the three possible exit channels for the second step, only 2a is favorable (i.e., slightly exothermic: -0.3 kcal/mol provided that the ZPE correction is taken into account) with respect

**Scheme 1. Relative Energies (kcal/mol) for the Interconversion of Tetramers (A =  $\text{Me}_4\text{Li}_4$ ; B =  $\text{Me}_3\text{Li}_4\text{Br}$ , C =  $\text{Me}_2\text{Li}_4\text{Br}_2$ , D =  $\text{MeLi}_4\text{Br}_3$ , E =  $\text{Li}_4\text{Br}_4$ )**



to  $(\text{MeLi})_2(\text{LiBr})_2$  and leads to  $(\text{MeLi})_3(\text{LiBr})$ . By contrast, both channels to  $(\text{MeLi})(\text{LiBr})_3$  (2b and 2c) are endothermic (by 0.9 and 2.1 kcal/mol, respectively) and are thus expected to be less efficient than path 2a, at least at low temperatures such as those at which the experiments were performed.

Therefore, these calculations account relatively well for the  $(\text{MeLi})_2(\text{LiBr})_2$  and  $(\text{MeLi})_3(\text{LiBr})$  proportions found experimentally as well as for the lower observed concentration for  $(\text{MeLi})(\text{LiBr})_3$  than is predicted by statistical arguments.

## Conclusion

The high-field, low-temperature NMR analysis of various mixtures of  $\text{Me}^6\text{Li}$  and  $^6\text{LiBr}$  in toluene gives access to all the  $^6\text{Li}$  signals of the  $(\text{MeLi})_n(\text{LiBr})_{4-n}$  aggregates. These have been unambiguously assigned using mono- and bidimensional (HOESY and COSY)

experiments. The  ${}^6\text{Li}$ – ${}^6\text{Li}$  coupling constants calculated by HF and DFT methods account relatively well for the observed correlations, although their values seem to be overestimated, probably due to the absence of solvent in the models considered. A comparable observation has been made before for the  $\text{MeLi}-(\text{Me}_2\text{O})_n$  aggregates: the  $J({}^{13}\text{C}$ – ${}^6\text{Li})$  decreases when going from  $n = 0$  to  $n = 3$ .<sup>19</sup> A slow ether exchange between the first solvation shell and the free diethyl ether in toluene has also been observed at low temperature. The relative variation of the concentration of these different aggregates in solution as a function of the  $\text{MeLi}/\text{LiBr}$  ratio has been determined. The data indicate that the populations of the complexes closely follow a pure statistical distribution, except for the  $\text{MeLi}(\text{LiBr})_3$  species, which is found to be less abundant than expected. The lower abundance of  $\text{MeLi}(\text{LiBr})_3$  could be rationalized on the aggregation energies computed using DFT, which suggests that the  $\text{MeLi}(\text{LiBr})_3$  complex is significantly less favored than the four other complexes. Large numerical differences between ZPE values associated with the different aggregates have been computed, due to the significant difference between the mass of the methyl group and that of the bromine atom. Therefore, this correction must be taken into account to obtain relevant enthalpies for reactions involving such systems.

Finally, this work suggests that working with  ${}^6\text{Li}$ -labeled compounds on high-field instruments can provide accurate information on the various species in solution. This can be of major importance in the understanding of the mechanisms and selectivities of reactions involving such reagents.

## Experimental Section

**Experimental Details.** Under an atmosphere of ultradry argon (dried and deoxygenated by bubbling through a com-

(13) The lithium amalgam was prepared in-house melting 0.5 g of commercially available  ${}^6\text{Li}$  (EurisoTop or Aldrich) with 2.5 mg of sodium in refluxing octadecane (317 °C) under strong magnetic stirring. The amalgamated metal was obtained as tiny spheres, quenching the flask at –40 °C. The octadecane was then melted by slightly warming the flask and filtering the lithium out.

(14) Kamienski, C. W.; Esmay, D. L. *J. Org. Chem.* **1960**, *25*, 1807.

(15) Duhamel, L.; Plaquevent, J.-C. *J. Organomet. Chem.* **1993**, *448*, 1.

(16) Frisch, M. J.; Trucks, G. W.; Schlegel, H. B.; Scuseria, G. E.; Robb, M. A.; Cheeseman, J. R.; Zakrzewski, V. G.; Montgomery, J. A.; Stratmann, R. E.; Burant, J. C.; Dapprich, S.; Millam, J. M.; Daniels, A. D.; Kudin, K. N.; Strain, M. C.; Farkas, O.; Tomasi, J.; Barone, V.; Cossi, M.; Cammi, R.; Mennucci, B.; Pomelli, C.; Adamo, C.; Clifford, F.; Ochterski, J.; Petersson, G. A.; Ayala, P. Y.; Cui, Q.; Morokuma, K.; Malick, D. K.; Rabuck, A. D.; Raghavachari, K.; Foresman, J. B.; Cioslowski, J.; Ortiz, J. V.; Stefanov, B. B.; Liu, G.; Liashenko, A.; Piskorz, P.; Komaromi, I.; Gomperts, R.; Martin, R. L.; Fox, D. J.; Keith, T.; Al-Laham, M. A.; Peng, C. Y.; Nanayakkara, A.; Gonzalez, C.; Challacombe, M.; Gill, P. M. W.; Johnson, B. G.; Chen, W.; Wong, M. W.; Andres, J. L.; Head-Gordon, M.; Replogle, E. S.; Pople, J. A. *Gaussian 98*, revision A7; Gaussian Inc.: Pittsburgh, PA, 1998.

(17) Wong, M. W.; Frisch, M. J.; Wiberg, K. B. *J. Am. Chem. Soc.* **1991**, *113*, 4776, and references therein.

(18) Helgaker, T.; Aa. Jensen, H. J.; Jørgensen, P.; Olsen, J.; Ruud, K.; Ågren, H.; Auer, A. A.; Bak, K. L.; Bakken, V.; Christiansen, O.; Coriani, S.; Dahle, P.; Dalskov, E. K.; Enevoldsen, T.; Fernandez, B.; Hättig, C.; Hald, K.; Halkier, A.; Heiberg, H.; Hetta, H.; Jonsson, D.; Kirpekar, S.; Kobayashi, R.; Koch, H.; Mikkelsen, K. V.; Norman, P.; Packer, M. J.; Pedersen, T. B.; Ruden, T. A.; Sanchez, A.; Saue, T.; Sauer, S. P. A.; Schimmelpfennig, B.; Sylvester-Hvid, K. O.; Taylor, P. R.; Vahtras, O. *DALTON, a molecular electronic structure program, release 1.2*; 2001. For the implementation of the calculation of spin–spin coupling constants, see also: (a) Vahtras, O.; Ågren, H.; Jørgensen, P.; Jensen, H. J. Aa.; Padkjaer, S. B.; Helgaker, T. *J. Chem. Phys.* **1992**, *96*, 6120. (b) Enevoldsen, T.; Oddershede, J.; Sauer, S. P. A., *Theor. Chem. Acc.* **1998**, *100*, 275.

mercial solution of *n*-butyllithium in hexane) at room temperature in distilled diethyl ether,  ${}^6\text{Li}$  (0.5% Na)<sup>13</sup> was reacted with methyl chloride.<sup>14</sup> A ~0.8–0.9 N salt-free MeLi solution was obtained (in about 50% yield) and assayed following usual procedures.<sup>15</sup> Various amounts of  ${}^6\text{LiBr}$  (previously prepared reacting HBr in diethyl ether with  $\text{Me}^6\text{Li}$  in the same solvent) were mixed with the methyl lithium, and 0.2 mmol of this ethereal solution (~220–250  $\mu\text{L}$ ) was then placed in the NMR tube and diluted to 0.9 mL with *d*<sub>8</sub>-toluene. Commercial tetrahydrofuran-*d*<sub>8</sub> was distilled over sodium and benzophenone.  ${}^6\text{Li}$  (95%) was purchased from Aldrich and washed in freshly distilled pentane.

**Computational Details.** All DFT energy calculations have been carried out using the Gaussian98<sup>16</sup> software with the B3P86 hybrid functional and 6-31+G\*\* basis set. For all systems, the geometries were fully optimized and the interaction energies reported take into account the zero-point vibrational corrections. The solvent (diethyl ether) was taken into account according to the self-consistent-field reaction scheme within the Onsager's dipole model.<sup>17</sup> All geometries were fully optimized and the zero-point energies (ZPE) were determined. The NMR Li–Li coupling constants in the various tetramers were calculated at the Hartree–Fock level with the same basis set using the Dalton<sup>18</sup> software. Our previous investigations have shown for tetramer A that correlation effects, as calculated from a MP2 treatment, on the coupling constants are small enough to be neglected.<sup>19</sup>

**Spectroscopical Details.** All NMR experiments were performed on a Bruker Avance DMX 500 spectrometer, equipped with a z-gradient unit and a 5 mm  $\{^1\text{H}, {}^6\text{Li}, {}^{13}\text{C}, \text{and } {}^{15}\text{N}\}$  quadruple-resonance Bruker probe. Measuring frequencies were 500 MHz ( ${}^1\text{H}$ ), 125 MHz ( ${}^{13}\text{C}$ ), and 73 MHz ( ${}^6\text{Li}$ ).  ${}^1\text{H}$  and  ${}^{13}\text{C}$  chemical shifts were referenced to the solvent *d*<sub>8</sub>-toluene signals at  $\delta$  2.09 and 20.40, respectively. Lithium spectra were referenced to external 0.3 M  ${}^6\text{LiCl}$  in  $\text{MeOH-}d_4$  ( $\delta$  0.0). Processing of NMR data was performed on an SGI O2 computer, using the manufacturer's program Xwinnmr2.1 (Bruker).

**1D NMR Measurements.** The proton and lithium one-dimensional data were recorded with standard parameters. To remove  ${}^{13}\text{C}$ – ${}^1\text{H}$  coupling, the one-dimensional  ${}^{13}\text{C}$  spectrum was recorded with broad band proton decoupling.

**2D NMR Measurements.  ${}^6\text{Li}/{}^6\text{Li}$  COSY.**<sup>20</sup> The following parameters were used for acquiring and processing the spectrum in absolute values: 128 experiments with 1024 data points and 8 scans each were recorded; a delay of evolution of long-range coupling of 250 ms was used; no proton decoupling was used; one time zero filling in  $f_1$ ; pure sine bell window function was applied before Fourier transformation.

**${}^6\text{Li}/{}^1\text{H}$  HOESY.**<sup>21</sup> The following parameters were used for acquiring and processing the spectrum in phase-sensitive mode: 128 experiments with 1024 data points and 16 scans each were recorded; pure phase line shapes was obtained by using time proportional phase incrementation (TPPI) phase cycling. A mixing time of 800 ms was used; one time zero filling in  $f_1$ ;  $\pi/2$  and  $\pi/3$  shifted sine square window functions were applied to  $f_2$  and  $f_1$  dimensions, respectively, before Fourier transformation.

**Acknowledgment.** The 500 MHz facility used in this study was supported by grants from the Conseil Régional de Haute-Normandie (France). We thank the Centre de Ressources Informatiques de Haute-Normandie (CRIHAN, Saint-Etienne-du-Rouvray) within

(19) Parisel, O.; Fressigné, C.; Maddaluno, J.; Giessner-Prettre, C. *J. Org. Chem.* **2003**, *68*, 1290.

(20) (a) Bax, A.; Freeman, R. *J. Magn. Reson.* **1981**, *44*, 542. (b) Günther, H.; Moskau, D.; Dujardin, R.; Maercker, A. *Tetrahedron Lett.* **1986**, *27*, 2251.

(21) Bauer, W.; Schleyer, P. v. R. *Magn. Reson. Chem.* **1988**, *26*, 827.

the framework of the “Bassin Parisien Régional Plan” (CPIBP) local modeling center for engineering sciences contract (article 12) and of the “Réseau Normand pour la Modélisation Moléculaire”, as well as the Centre de Calculs pour la Recherche (CCR, Université Pierre et Marie Curie, Paris). K.F. and S.D. received Ph.D.

stipends from the inter-regional RINCOF program and the Ministère de la Recherche et de la Technologie, respectively. We are grateful to Prof. Mark Tuckerman (New York University) for proofreading the manuscript.

OM030205R